# Negative mass effects of a spin soliton in Bose-Einstein condensates

Ling-Zheng Meng,[1] Shu-Wen Guan,[1] and Li-Chen Zhao[1,2,3,*]
[1]*School of Physics, Northwest University, Xi'an 710127, China*
[2]*NSFC-SPTP Peng Huanwu Center for Fundamental Theory, Xi'an 710127, China*
[3]*Shaanxi Key Laboratory for Theoretical Physics Frontiers, Xi'an 710127, China*

(Received 24 September 2021; accepted 23 December 2021; published 5 January 2022)

We investigate the energy-velocity dispersion relation of spin solitons with arbitrary initial velocities. Based on the dispersion relation, we further characterize the inertial mass of a spin soliton and find two critical velocities to distinguish between the positive mass and negative mass. One critical velocity separates the initial negative and positive masses, and the other denotes the velocity for negative-positive mass transition during an acceleration process. With the aid of the two critical velocities, we further propose two possible ways to observe the pure negative mass effect of a spin soliton. Moreover, the relations between the soliton's width and its velocity are discussed according to the variational results. We report that the soliton width can become narrower with larger moving speed (when a spin soliton possesses positive mass), in sharp contrast to the dark solitons reported before. These results would motivate experiments to observe negative mass effects of solitons in Bose-Einstein condensates.

DOI: 10.1103/PhysRevA.105.013303

## I. INTRODUCTION

Negative mass is an interesting subject [1–3] and is even believed to play a key role in stabilizing space-time wormholes and in explaining the supposed acceleration of the universe expansion [4]. Nowadays, negative mass is usually referred as the inertial mass emerging in solid physics and optical systems. Negative inertial mass is usually a direct consequence of the periodicity of the energy band structure [5,6], which has also been reported in the Bose-Einstein condensate (BEC) with periodic potentials [7,8]. BEC is also a good platform to study collective dynamics for its highly controllability. Recently, an experimental observation of negative mass effect was realized in BEC systems through engineering of the dispersion relation by spin-orbit coupling effects [9,10]. Besides this engineering of linear dispersion relations, nonlinearity was shown to induce negative mass [11]. Therefore, solitons induced by nonlinearity become a good candidate for observation on negative mass effects. The dark soliton [12] and magnetic soliton (a special dark-antidark soliton) [13,14] were suggested to admit negative mass properties in BEC systems.

However, it is difficult to directly drive dark solitons or antidark solitons by applying an external force, since those solitons have a nonzero density background [12–14]. Even the motion of a dark soliton in a harmonic trap suggested that it admitted negative mass [12,15–18], but we would like to observe negative mass effects of solitons (the accelerating direction is inverse to the force direction) by accelerating them more directly. We note that it is possible to drive a spin soliton by adding external forces on the bright soliton component in a two-component BEC system, since the spin soliton contains a bright soliton in one component and a dark soliton in the other component, and the the total density distribution is uniform [19]. In our previous studies, the spin soliton was shown to admit positive mass and negative mass periodically during an acceleration process [19]. There was a maximum speed for the spin soliton's acceleration process, which determined the negative-positive mass transition. Therefore, it is possible to investigate the pure negative mass of a spin soliton with some proper limitations on the moving speed. Moreover, the energy-velocity dispersion relation was used to explain the motion of a spin soliton, when the initial spin soliton is static relative to the mass background [19]. But the general dispersion relation (with arbitrary initial speed given by exact spin soliton solution) is still absent, which can be used to fully characterize the inertial mass of spin solitons.

In this paper, we systemically discuss the energy-velocity dispersion relation of spin solitons with arbitrary initial velocities, which is an important development of the results in [19]. Based on full analysis on the inertial mass of spin solitons, we find two critical velocities to distinguish the positive mass from negative mass. One critical velocity is for the initial soliton states, and the other denotes the velocity for negative-positive mass transition during an acceleration process. Then we propose two possible ways to observe pure negative mass effects of spin solitons by driving them directly. Driven by a slowly varying kink-shaped potential, a spin soliton moves against the force and "climbs up" to the position with larger potential energy. This character more directly shows the soliton's negative mass effects, in contrast to the motion of dark solitons or magnetic solitons in a harmonic trap [12,13,15–18]. The final velocity of the spin soliton can be controlled well by the potential energy possessed by the kink-shaped potential. A negative mass oscillator is proposed

*zhaolichen3@nwu.edu.cn

 

through loading a spin soliton in an antiharmonic potential. Decay of the soliton energy makes the oscillation amplitude become larger, in contrast to the smaller oscillation amplitude for the positive mass oscillator in a harmonic trap. These results would motivate some discussions about the inertial mass of solitons and experimental observations of the negative mass in BECs.

The paper is organized as follows. In Sec. II, we derive the energy-velocity dispersion relation of spin solitons with arbitrary initial velocities through combining the exact spin soliton solution and Lagrangian variational method. Based on this dispersion relation, we fully characterize the inertial mass of a spin soliton and find two critical velocities to separate the positive mass and negative mass. In Sec. III, we propose two possible ways to observe negative mass effects of spin solitons by adding forces on the bright soliton component. In Sec. IV, the relation between width and moving speed is discussed. The spin soliton with positive mass can become narrower with acceleration, which cannot be described by the exact spin soliton solution. Finally, we summarize our results in Sec. V.

## II. THE ENERGY-VELOCITY DISPERSION RELATION AND INERTIAL MASS OF A SPIN SOLITON

We consider a two-component BEC system which is tightly confined in the radial direction so that the radial characteristic length is smaller than the healing length and its dynamics is essentially one-dimensional [20]. Rescaling the atomic mass and Planck's constant to be 1, the dimensionless dynamical equations can be written as the following coupled model,

$$i\frac{\partial\psi_+}{\partial t} = -\frac{1}{2}\frac{\partial^2\psi_+}{\partial x^2} + (g_1|\psi_+|^2 + g_2|\psi_-|^2)\psi_+ + V_+(x)\psi_+, \tag{1a}$$

$$i\frac{\partial\psi_-}{\partial t} = -\frac{1}{2}\frac{\partial^2\psi_-}{\partial x^2} + (g_2|\psi_+|^2 + g_3|\psi_-|^2)\psi_- + V_-(x)\psi_-, \tag{1b}$$

where $x$ is the axial coordinate, and $\psi = (\psi_+, \psi_-)^T$ denotes the condensate wave function, where $\pm$ refers to the two components. The parameters $g_1$ and $g_3$ denote intraspecies interactions between the atoms in the components $\psi_+$ and $\psi_-$, respectively, and $g_2$ describes the interspecies interactions between the atoms. If $g_2 - g_1 > 0$, a spin soliton solution with $|\psi_+|^2 + |\psi_-|^2 = 1$ can be obtained when $g_1 + g_3 = 2g_2$ and $V_+(x) = V_-(x) = 0$ as follows [19], $\psi_+(x,t) = \sqrt{1-\frac{v^2}{c_s^2}}\,\mathrm{sech}[\sqrt{c_s^2 - v^2}(x - vt)]e^{\frac{1}{2}i[-g_1 t - g_2 t + 2v(x-vt)]}$, $\psi_-(x,t) = \{\sqrt{1-\frac{v^2}{c_s^2}}\tanh[\sqrt{c_s^2 - v^2}(x - vt)] + \frac{iv}{c_s}\}e^{-i(-g_1+2g_2)t}$, where $c_s = \sqrt{g_2 - g_1}$ denotes the maximum speed of exact spin soliton solutions. In this paper, we set the parameters to $g_1 = 1$, $g_2 = 2$, $g_3 = 3$ for simplicity, and in this case $c_s = 1$. We note that the large differences between interaction strengths are chosen to make the soliton more obvious, and they can be adjusted directly by scaling transformation. For the spin solitons, an external force (for instance, by applying magnetic fields) can be added solely to the bright soliton since its background density is zero. This character is absent for the dark soliton [15–18] or the magnetic soliton [13,14]. Namely, we choose proper $V_+(x)$ to drive the spin soliton while setting $V_-(x) = 0$. This enables us to test negative inertial mass effects by directly observing the motion of a spin soliton. The motion of the spin soliton is similar to the spin currents discussed in [21,22]. The acceleration of spin currents has not been discussed before. We would like to investigate the motion of a spin soliton driven by different external potentials. The concept of the inertial mass captures the response of a spin soliton to an applied force, encapsulating Newton's equations of quasiparticle dynamics. The inertial mass of the soliton has been used to explain the motion of the soliton widely [13,15,19,23,24]. The inertial mass of the soliton is usually defined based on the energy-velocity dispersion relation of solitons [19,23,24]. Therefore, we derive the energy-velocity dispersion relation of the spin soliton first, which can be used to develop a quasiparticle model to predict or explain well the spin soliton's motion.

From the exact spin soliton solution, we can calculate the energy of the spin soliton as $\sqrt{c_s^2 - v^2}$. However, this relation cannot be used to describe the acceleration process of a spin soliton, since the exact spin soliton solution just holds for arbitrary constant velocities. The particle number for the bright soliton or the dark soliton depends on its moving velocity; this naturally means that the exact spin soliton solution cannot describe any motion of spin solitons driven by external fields. This problem had been solved by the modified Lagrangian variational method [19,25]. Therefore, we introduce a simple linear potential into the bright soliton component, namely, $V_+(x) = -Fx$, and $V_-(x) = 0$, to derive the energy-velocity dispersion relation (see the Appendix for details). The energy-velocity dispersion relation is derived as

$$E_s = \frac{c_s^2}{2\sqrt{c_s^2 - v_0^2}} \pm \sqrt{\left(\frac{c_s^2}{2\sqrt{c_s^2 - v_0^2}}\right)^2 - v^2}. \tag{2}$$

In this way, we extend the analysis of initial static spin solitons to the cases with arbitrary initial velocities. The expression Eq. (2) manifests that the soliton energy has two branches, and the plus (minus) sign of the second term corresponds to the negative (positive) mass branch.

When the second term equals zero, the two branches intersect and thus a critical velocity for the negative-positive mass transition can be given in the form of

$$c_m = \sqrt{\frac{c_s^4}{4(c_s^2 - v_0^2)}}. \tag{3}$$

It is likewise the upper speed limit for a spin soliton with initial velocity $v_0$. The result also manifests that the spin soliton with nonzero initial velocities can still oscillate periodically in the presence of a constant force [19]. Furthermore, the upper speed limit $c_m$ is a variable quantity positively correlated with the initial velocity $v_0$ ($v_0 < c_s$). Thus, the velocity of an accelerated spin soliton is not confined by $c_s$, significantly distinguished from scalar dark solitons [12,15–18] or vector dark-bright solitons [26].

In particular, there exists a special case that the initial velocity is equal to $c_m$, which means the spin soliton is in the critical state of the negative-positive mass transition. Hence,

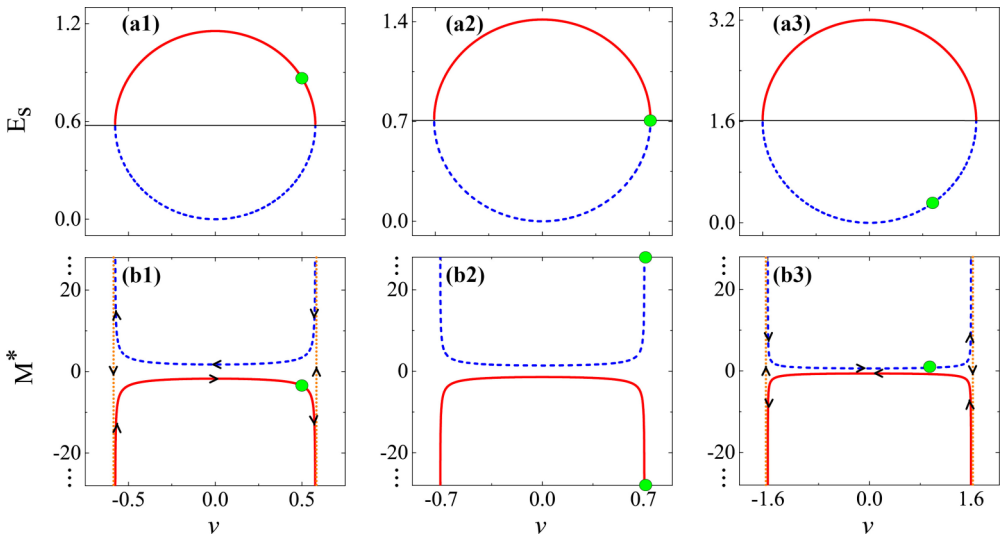


FIG. 1. Panel (a) shows the energy-velocity dispersion relations for spin solitons with three different initial velocities, (a1) $v_0 = 0.5$, (a2) $v_0 = v_{0c} = 1/\sqrt{2}$, and (a3) $v_0 = 0.95$. The solid red and dashed blue semicircles correspond to the negative and positive mass branches, respectively. The green dots denote the three initial states. It is seen that the initial velocity should be smaller than a critical value $v_{0c}$ for observing negative mass of the spin soliton. Panel (b) denotes the corresponding inertial mass of the spin solitons. The black arrows indicate the mass evolution of spin solitons driven by a linear potential $-Fx$ applying on the bright soliton. The parameters are $F = -0.01$, $g_1 = 1$, $g_2 = 2$, $g_3 = 3$.

the spin soliton with lower (higher) initial velocity admits negative (positive) mass. This critical velocity for the initial mass of spin solitons is derived as

$$v_{0c} = \frac{c_s}{\sqrt{2}}. \tag{4}$$

To gain insight into these two critical velocities, we plot several energy-velocity dispersion relations and the corresponding inertial mass for spin solitons with different initial velocities in Fig. 1. Evidently, a spin soliton with the initial velocity $v_0 = 0.5 < v_{0c}$ lies on the negative mass branch [solid red semicircle in Fig. 1(a1)]. For the spin soliton with the critical initial velocity $v_{0c}$, its initial state lies on the intersection of two branches [the transition point in Fig. 1(a2)]. If it has an initial velocity which is higher than $v_{0c}$, the initial state will locate at the positive mass branch [dashed blue semicircle in Fig. 1(a3)].

It must be stressed that the inertial mass of a spin soliton is different from the effective mass of a single particle [7,11]; it can be derived as the following form:

$$M^* = 2\frac{\partial E_s}{\partial(v^2)} = \mp\frac{m_0}{\sqrt{1-\frac{v^2}{c_m^2}}}, \tag{5}$$

where $m_0 = 2\sqrt{c_s^2 - v_0^2}/c_s^2$ denotes the soliton mass of the corresponding exact solution. When the initial velocity is zero, the soliton is static and $m_0$ is formally consistent with the rest mass in the theory of relativity. We note that in this case, the above relations are reduced to that in [19]. The corresponding inertial mass during the oscillation process is shown in the panel (b) of Fig. 1, for which the initial conditions are given by the exact spin soliton solution with different initial velocities, respectively. For the $v_0 = 0.5$ ($v_0 = 0.95$) case, the spin soliton first admits negative (positive) mass and later transits to positive (negative) mass [see Figs. 1(b1) and 1(b3)]. During this process, the soliton becomes heavier with the increase of velocity, its inertial mass tends to infinity, and the sign changes when $v = c_m$. The black arrows in Figs. 1(b1) and 1(b3) indicate the mass evolution of spin solitons driven by a linear potential $-Fx$, which is performed on the bright soliton component. Specifically, a spin soliton with the critical initial velocity $v_{0c}$ admits divergent mass [see Fig. 1(b2)]. This means that it possesses an infinite mass and its speed is hard to change. This character is supported by the numerical simulation results in next section.

We further consider the dynamics for a spin soliton subjected to a linear potential $V_+(x) = -Fx$. The external potential energy of the soliton is $E_p = \int_{-\infty}^{+\infty} -Fx|\psi_+|^2 dx = -2Fx_c\sqrt{c_s^2 - v_0^2}/c_s^2$ ($x_c$ denotes the soliton center position) under the local density approximation. From the energy conservation $E_s + E_p = \sqrt{c_s^2 - v_0^2}$ with the initial conditions $t = 0, x_c = 0, v = v_0$, we can derive the kinetic equation of the spin soliton as $\frac{d^2x_c}{dt^2} + 4F^2\frac{c_s^2 - v_0^2}{c_s^4}x_c + \frac{c_s^2 - 2v_0^2}{c_s^2}F = 0$. The motion of the spin soliton can be also given from the initial conditions. The derivation suggests that the periodic transition between negative and positive mass of the spin soliton driven by a constant force can be equivalently described by a harmonic oscillator. We can see that the results with $v_0 = 0$ reduce to the oscillation amplitude $A = \frac{c_s^2}{2|F|}$ and period $T = \frac{c_s\pi}{|F|}$ for an initial static spin soliton [19]. Our numerical simulations for the spin soliton driven by $F = -0.01$ agree well with the quasiparticle model. Both of them show a transition between infinite negative mass and positive mass, which is similar to the case in Bloch oscillation [27].

It should be noted that the energy-velocity dispersion relation holds for many other slowly varying potentials, although the linear potential is chosen to derive the relation for simplicity. Since the negative-positive mass transition effects

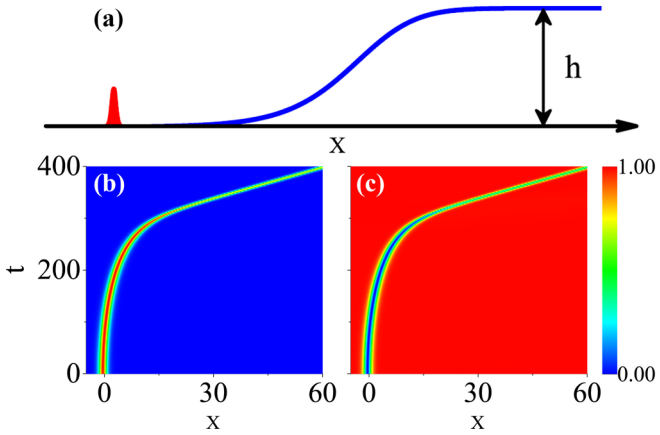


FIG. 2. (a) The profile schematic diagram of a kink-shaped potential. The numerical simulation results (b) and (c) for evolutions in two components when the potential is applied to the bright soliton. The spin soliton with a zero initial velocity accelerates in the direction opposite to the force. The parameters are $g_1 = 1, g_2 = 2, g_3 = 3, D = 0.995, h = 0.15$.

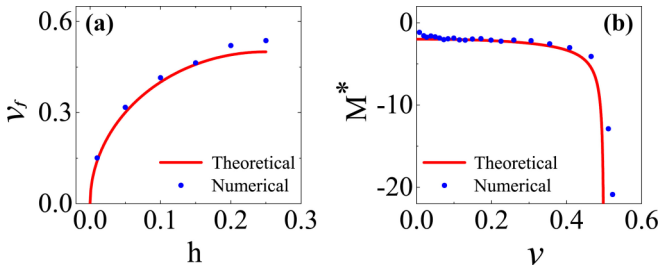


FIG. 3. (a) The final velocity of an initial static spin soliton versus the height of the kink-shaped potential. The numerical results (blue dots) are obtained with different heights $h = 0.01, 0.05, 0.1, 0.15, 0.2, 0.25$. (b) The relation between inertial mass of a spin soliton and its moving velocity. The blue dots are obtained from numerical simulation with $h = 0.25$. The quasiparticle theory gives the red solid line. It is seen that the quasiparticle theory can explain well the numerical results. The other parameters are $g_1 = 1, g_2 = 2, g_3 = 3, D = 0.995$.

have been discussed before [19], we mainly investigate the pure negative mass effect of a spin soliton, with the aid of full dispersion relation and the two critical velocities.

## III. THE PURE NEGATIVE MASS OF SPIN SOLITON

We can observe the pure negative mass of the spin soliton by adding slowly varying potentials on the bright soliton component. Taking two cases as examples, we choose a kink-shaped potential and an antiharmonic potential to demonstrate the negative mass effects.

### A. Controllable motion of spin soliton with negative mass

We first use a kink-shaped potential to drive the spin soliton. The potential is chosen as $V_+(x) = \frac{h}{4}(\tanh[-\sqrt{1-D^2}x] - 1)^2$, where $D$ controls the slope and $h$ denotes the height of a kink-shaped potential. We choose a large value of $|g_2 - g_1|$ to decrease the soliton width and choose an appropriate value of $D$ to ensure that the potential varies slowly on the size scale of the soliton. In addition, the height $h$ should be lower than an upper limit to avoid accelerating the spin soliton to the positive mass region, since the sign of inertial mass would change when its velocity reaches $c_m$. This weak potential is only added to the bright soliton component $\psi_+$ to eliminate the acceleration of the entire particle density background. We have an initially static spin soliton ($v_0 = 0$) at the bottom of the potential. The profile schematic diagram is shown in Fig. 2(a). Then the spin soliton is naturally expected to "climb up" to the top of this kink-shaped potential due to the negative mass effect.

We made the numerical simulations by the integrating-factor method together with a fourth-order Runge-Kutta method to test this anomalous behavior, and the exact spin soliton solution given above can be a perfect initial condition for our simulation. The results of the two components are shown in Figs. 2(b) and 2(c). The external potential forms an accelerating field that can apply a force on the soliton in the direction of the lower potential. Strikingly, the acceleration of the static spin soliton is opposite to the direction of the force. This surprising dynamical behavior directly demonstrates the negative mass property of the spin soliton, and provides us with a way to manipulate solitons with negative mass. According to energy conservation and the energy-velocity dispersion relation of spin solitons, we obtain the quantitative relation between the potential height $h$ and the final soliton velocity $v_f$ (after climbing up the kink potential) as follows:

$$\frac{c_s^2}{2\sqrt{c_s^2 - v_0^2}} + \sqrt{\left(\frac{c_s^2}{2\sqrt{c_s^2 - v_0^2}}\right)^2 - v_f^2} + \frac{2h\sqrt{c_s^2 - v_0^2}}{c_s^2} = \sqrt{c_s^2 - v_0^2}. \tag{6}$$

The soliton energy term is chosen as the negative mass branch in the above expression. The $v_0$ is an arbitrary initial velocity given by exact spin soliton solution, and it should be smaller than the critical initial velocity $v_{0c}$. Moreover, the potential height $h$ is also limited for observing the pure negative mass effect, whose value is given by initial velocity and the other critical velocity $c_m$. When the initial velocity of the soliton is zero, the upper limit of the potential height is $h = c_s^2/4$, for observing the pure negative mass effect. Then the relation between the height $h$ and the final velocity $v_f$ can be obtained theoretically [red line in Fig. 3(a)]. The theoretical as well as numerical results show that the initial static spin soliton was accelerated by different kink-shaped potentials and the final velocities are predicted well by our theoretical results.

The motion of spin solitons under different potential heights in Fig. 3(a) indicates that the spin soliton indeed admits negative mass. For instance, we show the variation of the spin soliton's inertial mass during the acceleration process in Fig. 3(b), where the potential height is chosen as 0.25. The velocity of the spin soliton slightly exceeds the theoretical limit derived by Eq. (6), due to that the soliton energy decays during the acceleration process.

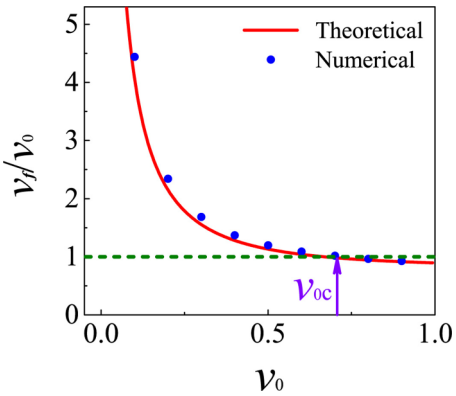


FIG. 4. The relation between the ratio of the soliton's final and initial velocity versus its initial velocity. The numerical results (blue dots) are obtained from the spin soliton crossing the kink-shaped potential with different initial velocities. The quasiparticle theory gives the red solid line theoretically. The green dashed line indicates the case of $v_f = v_0$, which can be used to distinguish the acceleration or deceleration of the spin soliton. The parameters are $g_1 = 1, g_2 = 2, g_3 = 3, D = 0.995, h = 0.1$.

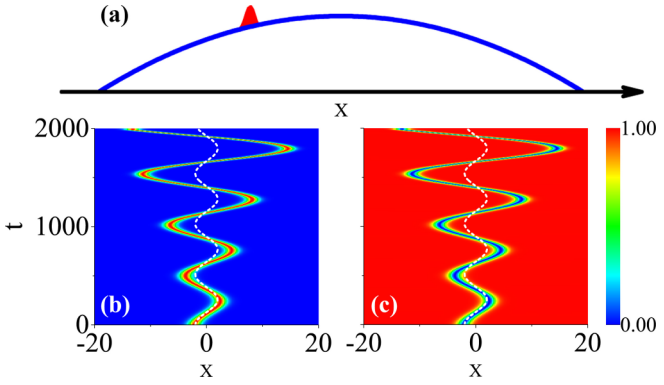


FIG. 5. (a) The profile schematic diagram of the initial soliton in antiharmonic potential. The numerical simulation results (b) and (c) show that the spin soliton oscillates periodically with the amplitude getting larger. The white dashed line denotes the oscillation described by the quasiparticle theory. The distance between the initial soliton and the center of the potential is $\Delta x = -2$; other parameters are $g_1 = 1, g_2 = 2, g_3 = 3, \omega = 0.012$.

On the other hand, the motion of spin solitons with different initial velocities can be used to test the above theoretical prediction on $v_{0c}$. For the solitons with nonzero initial velocities, we introduce the ratio $v_f/v_0$ to depict the change of the solitons' motion, which can be used to denote the inertial mass character of spin solitons. If $v_f/v_0 > 1$, this means that the acceleration and spin soliton admit negative mass; if $v_f/v_0 < 1$, the spin soliton admits positive mass. We simulated the evolutions of spin solitons with different initial velocities. The slope and height of the potential are fixed to $D = 0.995$ and $h = 0.1$. The numerical results are shown as blue dots in Fig. 4. Theoretical result is denoted by the red solid line, which is given by the energy conservation and the energy-velocity dispersion relation of spin solitons. One can see that $v_{0c}$ indeed distinguishes well between the initial negative and positive masses.

Particularly, if the initial velocity $v_0 = v_{0c}$, we have $v_f/v_0 = 1$ theoretically. Figure 4 shows that the spin soliton keeps nearly the same velocity after crossing the kink-shaped potential. This character partly supports the above predicted divergent mass character at the critical initial velocity [see Fig. 1(b2)]. It should be noted that the divergent mass cannot be shown well for much larger potential height $h$, since energy conservation and continuous increase of the bright soliton's external potential energy break the critical soliton state.

### B. The oscillation of a spin soliton in antiharmonic potentials

It is known that a substance with positive inertial mass can oscillate periodically in a harmonic potential, while the negative mass effect of the spin soliton allows it to have anomalous kinetic effects. Hence, it can be expected that when we put the spin soliton in an antiharmonic potential, it could show a similar oscillating behavior. Taking the antiharmonic potential $V_+(x) = -\frac{1}{2}\omega^2 x^2$ as an example, a spin soliton is placed closely to the center of the potential [see Fig. 5(a)]. Simulating the Eq. (1) numerically, we see that the spin soliton begins to move toward the top of potential which is caused by its negative mass effects, and then oscillates periodically to form a negative mass oscillator, shown in Figs. 5(b) and 5(c).

The above general energy-velocity dispersion relation can be used to explain the oscillation of spin solitons in the antiharmonic potential. If the potential varies slowly within the soliton size scale, the local density approximation gives $\int_{-\infty}^{\infty} -\frac{1}{2}\omega^2 x^2 |\psi_+|^2 dx \approx -\frac{1}{2}\omega^2 x_c^2 \int_{-\infty}^{\infty} |\psi_+|^2 dx$. Based on the conservation of energy $\frac{c_s}{2} + \sqrt{\frac{c_s^2}{4} - v^2} + \int_{-\infty}^{\infty} -\frac{1}{2}\omega^2 x^2 |\psi_+|^2 dx = c_s$, the dynamical equation of the spin soliton's center is derived:

$$\frac{\partial^2 x_c}{\partial t^2} + 2\omega^2 x_c \sqrt{\frac{1}{4} - \left(\frac{\partial x_c}{\partial t}\right)^2} = 0. \tag{7}$$

If the soliton is placed closely to the center of potential, its velocity is always small, i.e., $\frac{\partial x_c}{\partial t} = v \approx 0$. The above equation predicts that the soliton will oscillate with period $T \approx 2\pi/\omega$. In fact, the oscillation period could be a bit larger than $T$. This is quite different from the oscillation period of a dark soliton [12,18] or a dark-bright soliton [28] in a harmonic potential. Although it is hard to derive the exact oscillation period from Eq. (7), we can solve it numerically with initial conditions. The quasiparticle theory predicts the white dashed curves in Fig. 5. The density evolution of the spin soliton indicates that the oscillating period agrees well with the theoretical results. But the amplitude of the oscillator increases gradually due to the decay of the soliton energy. It should be noted that the soliton cannot be placed far away from the potential center; otherwise the harmonic oscillation will be destroyed.

## IV. ANOMALOUS CORRELATION BETWEEN WIDTH AND VELOCITY OF SPIN SOLITON

Generally, the widths of scalar dark solitons [12,15–18] or vector dark-bright solitons [26] are positively correlated with their velocities.

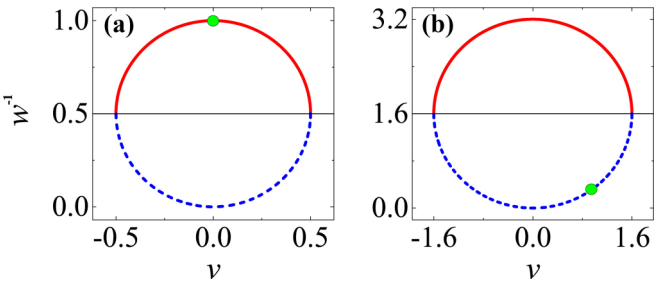


FIG. 6. The relations between width and velocity of spin solitons with initial velocities (a) $v_0 = 0$ and (b) $v_0 = 0.95$. The solid red and dashed blue semicircles correspond to negative and positive mass regions, respectively. The green dots denote the initial states. The width of a spin soliton with negative mass is positively correlated with its speed, whereas for the positive mass one, the relation is reversed.

Recent research on the negative-positive mass transition of spin solitons [19] reveals that this correlation is only applicable to the negative mass region. During the ac oscillation [19], one can directly find that when the spin soliton reaches the maximum displacement, it is widest but the velocity decreases to zero; namely the spin soliton did not return to its original state. This anomalous effect indicates that the inertial mass significantly impacts the variation of soliton width with velocity. Very recently, a similar property of a magnetic domain wall was reported in ferromagnetic spin-1 BECs [29]. Based on the derivation of spin soliton's velocity $v$ and width $w$ (as functions of time) in the Appendix, we have the soliton width-velocity relation as

$$w^{-1} = \frac{c_s}{2\sqrt{c_s^2 - v_0^2}} \pm \sqrt{\frac{c_s^2}{4(c_s^2 - v_0^2)} - \frac{v^2}{c_s^2}}. \tag{8}$$

It is quite explicit that the width $w$ is not a monotonic function of the velocity $v$. Particularly, this indicates that spin solitons with different inertial mass admit opposite width-velocity relations.

We show the width-velocity relation of spin solitons with two different initial velocities in Fig. 6. The semicircles correspond to the negative (solid red line) and positive (dashed blue line) mass of spin solitons, respectively. For an initial soliton with negative mass, the spin soliton's width will widen when its moving speed is increased. This character is consistent with the upper semicircle in Fig. 6(a). By contrast, if it reaches the maximum speed and transits to the positive mass region, the width-velocity relation will be reversed.

For the spin soliton with initial positive mass, i.e., the initial velocity $v_0 > v_{0c}$, a width-velocity relation is shown in Fig. 6(b) as an example. The initial state lies on the lower semicircle which corresponds to the positive mass, and its width narrows as its speed increases. Moreover, it can be seen in Fig. 6(b) that a spin soliton with the initial positive mass can be accelerated and exceeds $c_s$, where $c_s = \sqrt{g_2 - g_1}$ is the maximum speed given by the exact spin soliton solution. Thus the velocity of an accelerated spin soliton is limited by $c_m$ rather than $c_s$. This shocking phenomenon is also described well by the energy-velocity dispersion relation.

## V. CONCLUSION AND DISCUSSION

We derive the energy-velocity dispersion relations of spin solitons through combining the exact spin soliton solution and Lagrangian variational method. The negative and positive masses of spin solitons are clarified systemically based on the two critical velocities. A critical velocity $v_{0c}$ distinguishes between the initial negative mass and positive mass, and the other velocity $c_m$ signifies the negative-positive mass transition during the acceleration process. Our general energy-velocity dispersion relations of spin solitons enable us to describe well the motion of an accelerated spin soliton driven by slowly varying external potentials, although the dispersive wave and sound wave induce weak decay of the soliton energy. Two possible ways are suggested to observe the negative mass of a spin soliton. Moreover, we demonstrate that the dark soliton's width can become narrower with larger moving speed, when a spin soliton possesses positive mass. This character is usually absent for the dark solitons reported before [12,15,17,20,30]. The dispersion relation and negative mass of spin solitons could be tested in a two-component BEC, since magnetic solitons (similar to spin solitons) were observed recently in experiments [31,32].

## ACKNOWLEDGMENTS

This work is supported by the National Natural Science Foundation of China (Contracts No. 12022513, No. 11775176, No. 11947301, and No. 12047502) and the Major Basic Research Program of Natural Science of Shaanxi Province (Grants No. 2018KJXX-094 and No. 2017KCT-12).

## APPENDIX: THE MOTION OF SPIN SOLITON WITH NONZERO INITIAL MOVING VELOCITY

In the presence of the force $F$ term, the exact analytic expressions for the dynamic evolution of the spin solitons cannot be obtained. We thus exploit the Lagrangian variational method to evaluate the dynamics of the spin soliton by introducing the following trial functions,

$$\psi_+(X,T) = f(T)\,\mathrm{sech}\left[\frac{X - b(T)}{w(T)}\right] e^{i\phi_0(T) + i\phi_1(T)[X - b(T)]}, \tag{A1a}$$

$$\psi_-(X,T) = \left\{ i\sqrt{1 - f(T)^2} + f(T)\tanh\left[\frac{X - b(T)}{w(T)}\right]\right\} e^{i\theta_0(T)}, \tag{A1b}$$

where $X = c_s x$ and $T = c_s^2 t$ are introduced to simplify the following calculations. Note that the total density keeps a constant during temporal evolution, while the soliton position, amplitudes, and width vary in time. This is distinctive from the case in [26]. We now use the Lagrangian variational method to derive expressions of $b(T)$, $f(T)$, $w(T)$, $\phi_1(T)$, $\phi_0(T)$, $\theta_0(T)$. The Lagrangian of

the system is

$$L(T)=\int_{-\infty}^{+\infty}\left\{c_s\left[\frac{i}{2}(\psi_+^*\partial_T\psi_+-\psi_+\partial_T\psi_+^*)+\frac{i}{2}(\psi_-^*\partial_T\psi_--\psi_-\partial_T\psi_-^*)\left(1-\frac{1}{|\psi_-|^2}\right)-\frac{1}{2}|\partial_X\psi_+|^2-\frac{1}{2}|\partial_X\psi_-|^2\right]\right.$$
$$\left.-\frac{1}{c_s}\left[\frac{g_1}{2}|\psi_+|^4+\frac{g_3}{2}(|\psi_-|^2-1)^2+g_2|\psi_+|^2(|\psi_-|^2-1)\right]+\frac{1}{c_s^2}FX|\psi_+|^2\right\}dX. \tag{A2}$$

The factor $(1-\frac{1}{|\psi_-|^2})$ was first introduced in [25] for the integration of the dark soliton state. Substituting the trial wave functions into the Lagrangian, and after taking the particularly elaborate integrals, we obtain that

$$L(T)=c_s\left\{2f(T)^2w(T)[\phi_1(T)b'(T)-\phi_0'(T)]-\frac{f(T)^2}{w(T)}[1+\phi_1(T)^2w(T)^2]+2f(T)^2w(T)\theta_0'\right.$$
$$\left.+2b'(T)\arcsin[f(T)]-2b'(T)f(T)\sqrt{1-f(T)^2}\right\}+\frac{1}{c_s^2}2Ff(T)^2w(T)b(T), \tag{A3}$$

where $b'(T)=\frac{d}{dT}b(T)$, etc.

Differently from the ones for an initial static spin soliton [19], we consider a more general case for which the initial conditions are given by the exact spin soliton solution with arbitrary initial velocities. This will require that our initial conditions for the trial wave functions be $f(0)=\sqrt{1-v_0^2/c_s^2}$, $w(0)=c_s/\sqrt{c_s^2-v_0^2}$, $b(0)=0$, $b'(0)=v_0/c_s$. From the conservation of the norm of the bright component, we have

$$w(T)=\frac{\sqrt{c_s^2-v_0^2}}{c_sf(T)^2}. \tag{A4}$$

Then it is straightforward to apply the Lagrangian equation $\frac{d}{dT}(\frac{\partial L(T)}{\partial\alpha'})=\frac{\partial L(T)}{\partial\alpha}$, where $\alpha=b(T),f(T),\phi_1(T),\phi_0(T),\theta_0(T)$. Using the initial conditions, we find the following solutions,

$$f(T)=\sin\left(\frac{\sqrt{c_s^2-v_0^2}}{c_s^4}FT+\delta\right), \tag{A5a}$$

$$b(T)=\pm\frac{c_s^5}{2F(c_s^2-v_0^2)}\sin^2\left(\frac{\sqrt{c_s^2-v_0^2}}{c_s^4}FT+\delta\right), \tag{A5b}$$

$$\phi_1(T)=\pm\frac{c_s}{2\sqrt{c_s^2-v_0^2}}\sin\left(2\frac{\sqrt{c_s^2-v_0^2}}{c_s^4}FT+2\delta\right), \tag{A5c}$$

where $\delta=\arcsin[\sqrt{1-v_0^2/c_s^2}]$.

Substituting the trial functions into the kinetic energy of the spin soliton, we obtain that

$$E_k=\int_{-\infty}^{+\infty}\left[\psi_+^*\left(-\frac{1}{2}\partial_x^2\right)\psi_++\psi_-^*\left(-\frac{1}{2}\partial_x^2\right)\psi_-\right]dx$$
$$=\frac{c_s^2}{\sqrt{c_s^2-v_0^2}}\sin^2\left(\frac{\sqrt{c_s^2-v_0^2}}{c_s^4}FT+\delta\right). \tag{A6}$$

The interaction energy can be also calculated as

$$E_{\text{inter}}=\int_{-\infty}^{+\infty}\left[\frac{g_1}{2}|\psi_+|^4+\frac{g_3}{2}(|\psi_-|^2-1)^2\right.$$
$$\left.+g_2|\psi_+|^2(|\psi_-|^2-1)\right]dx=0. \tag{A7}$$

Then the soliton energy $E_s=E_k+E_{\text{inter}}$. Moreover, the soliton's velocity evolves as

$$v=\frac{1}{c_s}\frac{db(T)}{dt}=\pm\frac{c_s^2}{2\sqrt{c_s^2-v_0^2}}\sin\left(2\frac{\sqrt{c_s^2-v_0^2}}{c_s^4}FT+2\delta\right). \tag{A8}$$

Based on these expressions for the soliton energy and moving velocity, we can finally obtain the energy-velocity dispersion relation, and the relation can be further used to calculate the inertial mass of a spin soliton.


[1] H. Bondi, Negative mass in general relativity, Rev. Mod. Phys. **29**, 423 (1957), and references therein.

[2] H. Kromer, Proposed negative-mass microwave amplifier, Phys. Rev. **109**, 1856 (1958).

[3] W. B. Bonnor and F. I. Cooperstock, Does the electron contain negative mass? Phys. Lett. A **139**, 442 (1989).

[4] J. P. Petit and G. d'Agostini, Negative mass hypothesis in cosmology and the nature of dark energy, Astrophys. Space Sci. **354**, 611 (2014).

[5] F. Bloch, Quantum mechanics of electrons in crystal lattices, Z. Phys. **52**, 555 (1928).

[6] C. Zener, A theory of the electrical breakdown of solid dielectrics, Proc. R. Soc. London, Ser. A **145**, 523 (1934).

[7] M. B. Dahan, E. Peik, J. Reichel, Y. Castin, and C. Salomon, Bloch Oscillations of Atoms in an Optical Potential, Phys. Rev. Lett. **76**, 4508 (1996).

[8] H. Sakaguchi and B. A. Malomed, Interactions of solitons with positive and negative masses: Shuttle motion and coacceleration, Phys. Rev. E **99**, 022216 (2019).

[9] M. A. Khamehchi, K. Hossain, M. E. Mossman, Y. Zhang, T. Busch, M. M. Forbes, and P. Engels, Negative-Mass Hydrodynamics in a Spin-Orbit-Coupled Bose-Einstein Condensate, Phys. Rev. Lett. **118**, 155301 (2017).

[10] D. Colas, F. P. Laussy, and M. J. Davis, Negative-Mass Effect in Spin-Orbit Coupled Bose-Einstein Condensates, Phys. Rev. Lett **121**, 055302 (2018).

[11] F. DiMei, P. Caramazza, D. Pierangeli, G. DiDomenico, H. Ilan, A. J. Agranat, P. DiPorto, and E. DelRe, Intrinsic Negative Mass from Nonlinearity, Phys. Rev. Lett. **116**, 153902 (2016).

[12] Th. Busch and J. R. Anglin, Motion of Dark Solitons in Trapped Bose-Einstein Condensates, Phys. Rev. Lett. **84**, 2298 (2000).

[13] C. Qu, L. P. Pitaevskii, and S. Stringari, Magnetic Solitons in a Binary Bose-Einstein Condensate, Phys. Rev. Lett. **116**, 160402 (2016).

[14] C. Qu, M. Tylutki, S. Stringari, and L. P. Pitaevskii, Magnetic solitons in Rabi-coupled Bose-Einstein condensates, Phys. Rev. A **95**, 033614 (2017).

[15] A. Muryshev, G. V. Shlyapnikov, W. Ertmer, K. Sengstock, and M. Lewenstein, Dynamics of Dark Solitons in Elongated Bose-Einstein Condensates, Phys. Rev. Lett. **89**, 110401 (2002).

[16] L. M. Aycock, H. M. Hurst, D. K. Efimkin, D. Genkina, H.-I. Lu, V. M. Galitski, and I. B. Spielman, Brownian motion of solitons in a Bose–Einstein condensate, Proc. Natl. Acad. Sci. USA **114**, 2503 (2017).

[17] H. M. Hurst, D. K. Efimkin, I. B. Spielman, and V. Galitski, Kinetic theory of dark solitons with tunable friction, Phys. Rev. A **95**, 053604 (2017).

[18] V. N. Serkin, Busch-Anglin effect for matter-wave and optical dark solitons in external potentials, Optik **173**, 1 (2018).

[19] L.-C. Zhao, W. Wang, Q. Tang, Z.-Y. Yang, W. Yang, and J. Liu, Spin soliton with a negative-positive mass transition, Phys. Rev. A **101**, 043621 (2020).

[20] P. G. Kevrekidis, D. J. Frantzeskakis, and R. Carretero-Gonzalez, *Emergent Nonlinear Phenomena in Bose-Einstein Condensates: Theory and Experiment* (Springer, Berlin, 2008).

[21] Q. Z. Zhu, Q. F. Sun, and B. Wu, Superfluidity of a pure spin current in ultracold Bose gases, Phys. Rev. A **91**, 023633 (2015).

[22] J. H. Kim, S. W. Seo, and Y. Shin, Critical Spin Superflow in a Spinor Bose-Einstein Condensate, Phys. Rev. Lett. **119**, 185302 (2017).

[23] R. G. Scott, F. Dalfovo, L. P. Pitaevskii, and S. Stringari, Dynamics of Dark Solitons in a Trapped Superfluid Fermi Gas, Phys. Rev. Lett. **106**, 185301 (2011).

[24] S. S. Shamailov and J. Brand, Quasiparticles of widely tuneable inertial mass: The dispersion relation of atomic Josephson vortices and related solitary waves, SciPost Phys. **4**, 018 (2018).

[25] Y. S. Kivshar and W. Królikowski, Lagrangian approach for dark solitons, Opt. Commun. **114**, 353 (1995).

[26] M. O. D. Alotaibi and L. D. Carr, Dynamics of dark-bright vector solitons in Bose-Einstein condensates, Phys. Rev. A **96**, 013601 (2017).

[27] Z. A. Geiger, K. M. Fujiwara, K. Singh, R. Senaratne, S. V. Rajagopal, M. Lipatov, T. Shimasaki, R. Driben, V. V. Konotop, T. Meier, and D. M. Weld, Observation and Uses of Position-Space Bloch Oscillations in an Ultracold Gas, Phys. Rev. Lett. **120**, 213201 (2018).

[28] Th. Busch and J. R. Anglin, Dark-Bright Solitons in Inhomogeneous Bose-Einstein Condensates, Phys. Rev. Lett. **87**, 010401 (2001).

[29] X. Yu and P. B. Blakie, Anomalous dynamics of magnetic field-driven propagating magnetic domain walls, arXiv:2104.12967.

[30] R. Liao and J. Brand, Traveling dark solitons in superfluid Fermi gases, Phys. Rev. A **83**, 041604(R) (2011).

[31] A. Farolfi, D. Trypogeorgos, C. Mordini, G. Lamporesi, and G. Ferrari, Observation of Magnetic Solitons in Two-Component Bose-Einstein Condensates, Phys. Rev. Lett. **125**, 030401 (2020).

[32] X. Chai, D. Lao, K. Fujimoto, R. Hamazaki, M. Ueda, and C. Raman, Magnetic Solitons in a Spin-1 Bose-Einstein Condensate, Phys. Rev. Lett. **125**, 030402 (2020).